

Variation of the NRCS of the Sea with Increasing Roughness

NORMAN W. GUINARD, JOHN T. RANSONE, JR., AND JOHN C. DALEY

Naval Research Laboratory, Washington, D. C. 20390

Recently a new model for the normalized radar cross section (NRCS) of the sea has been developed that is based on the scattering from a composite surface, i.e., one in which a slightly rough surface in the sense of Rice has been superimposed upon a large wave structure. The model predicts an upper bound (saturation value) of the NRCS with increasing wind speed and in addition yields expressions for the variation of the NRCS with frequency, polarization, and grazing angle. To verify the validity of the model in the higher sea states where spray, shadowing, and nonlinear wave interactions would be expected to influence the return, extensive measurements were made over the North Atlantic Ocean in February 1969. The instrumentation used in the program was the Naval Research Laboratory four-frequency radar system which is an experimental radar installed in an EC-121 (Super Constellation) aircraft. Nine flights were made, and data acquired in sea states with winds that varied from Beaufort Force 0 to 8 with a maximum sea state condition of a 24-m/sec wind with 8.5-meter significant wave height were observed. The results of the measurement have verified the existence of the upper bound for the NRCS that is asymptotically approached in windspeeds in excess of 5 m/sec. In addition, the data have confirmed the variation of the cross section with frequency, polarization, and grazing angle with the proviso that the 'tilting' of the scattering surface by the large wave structure be assumed in the region of shallow grazing angles.

Great interest has recently been aroused in the radar community in the variation of the normalized radar cross section (NRCS) of the sea with increasing ocean roughness. There are three reasons for this sudden change in a field of study which has lain relatively dormant for more than a decade. First, the impetus provided by the continuing development of long-range ocean surveillance techniques has made the description of clutter backgrounds in terms of a worst-case condition an increasingly important requirement for specification and design of radar systems. Second, the application of active radar in the remote sensing of local wind fields and sea state or both has made knowledge of the variation of the NRCS with wind a prime requisite for system feasibility studies. Third, a new model for sea clutter has been developed by several scientists working in both the United States and the Soviet Union that offers new insights into the mechanisms of the scattering of radar signals from the sea surface and therefore provides a theoretical base from which both the worst-case clutter condition and the variation of NRCS with wind and sea state may be inferred.

The Naval Research Laboratory has been investigating radar sea return for many years by using the four-frequency radar (4FR) system which is an airborne coherent pulsed radar that is capable of transmitting a sequence of four frequencies, *X* band (8910 MHz), *C* band (4455 MHz), *L* band (1228 MHz), *P* band/UHF (428 MHz) alternately on horizontal and vertical polarization. These correspond to transmitted wavelengths of approximately 3, 6, 24, and 70 cm respectively. For a detailed description of this unique instrumentation, see *Guinard* [1969]. It was natural because of these developments that a new study be initiated to verify and to expand the utility of the model by collating it with cross-sectional measurements made with this combination of transmitted signals over a wide variety of sea conditions. This study, reviewed by *Guinard and Daley* [1970], primarily used data obtained with the 4FR system in low and moderate sea states in the vicinity of Puerto Rico in July 1965. The results of the comparison, in addition to establishing the validity of the new model for ocean application, strongly indicated the need to definitively measure the sea return in high-sea states where nonlinear effects such as shadowing, spray, and foam might tend to limit its effectiveness. Conse-

quently, measurements were made over the North Atlantic Ocean in February 1969 that have yielded data whose implication strongly affects both radar surveillance and remote-sensing system design. Before describing the North Atlantic experiment and presenting some of the more relevant data, it is necessary to briefly discuss the composite surface model to place the measurement program in context and because the model provides a powerful oceanographic tool for the investigation of dynamic processes at the ocean surface.

THE COMPOSITE SURFACE MODEL

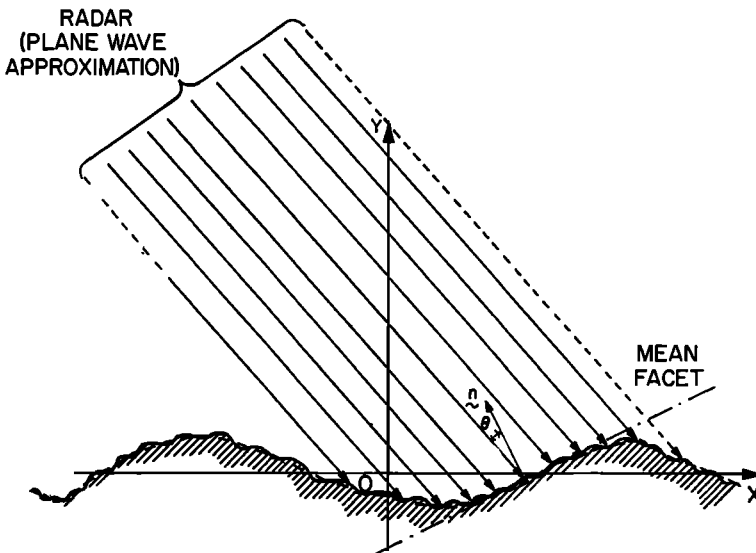
The new model, formulated independently by Wright [1968] and by Bass *et al.* [1968] (their bibliography gives an excellent listing of Soviet efforts in the evolution of the model), treats the energy backscattered from the sea surface at angles in which the reflection from the facets oriented nearly normal to the direction of the incident radiation has a zero probability. In the model, the sea surface is a composite similar to that studied by Semyonov [1966] and Barrick and Peake [1968]. It consists of waves extremely long compared with the radar wavelength on which a smaller wave structure is superimposed (Figure 1). The smaller structure in turn is composed of short gravity and capil-

lary waves of length comparable to the radar wavelength which together comprise the scattering surface. The long waves produce a 'tilting' of the scattering surface and thus modify the direction of incidence of the illuminating signal.

This apparently arbitrary division of the continuous ocean-wave spectrum has a physical basis. In 1912, Bragg observed, in his studies of X-ray crystallography, that when a beam of monochromatic X rays is incident on a crystal face at an angle off the normal, the reflection from the successive sheets of atoms in the crystal is a maximum when the path length difference is an integral number of wavelengths. A similar principle is widely used in geometric optics. To restate Bragg's Law for radar scattering, the return from an equally spaced array of point scatterers (Figure 2) will be a maximum when the respective path length differences are an integral number of half wavelengths; i.e., when the scattering centers are spaced in the plane of the incident wave of length λ_r at a distance

$$L = \frac{m\lambda_r}{2} \sec \gamma \quad m = 1, 2, \dots \quad (1)$$

For first-order Bragg scattering, this leads to the wave number relationship



COMPOSITE ROUGH SURFACE

Fig. 1. Composite rough surface.

$$K = 2\beta \cos \gamma = 2\beta \sin \theta \quad (2)$$

where θ is the angle of incidence, and K and β are the wave numbers of the array spacing and incident energy, respectively. The return from a random array of scatterers will thus be primarily a measure of the scattering strength of those points whose spacing satisfies the condition in equation 1. Extending the concept of Bragg scattering to a sinusoidal surface periodic with length L and wave amplitude $P < \lambda_r$, it is obvious that the scattering will be maximum when the path length differences from the source to points A and A' , and B and B' , are integral numbers of half wavelengths so that L again must satisfy the Bragg condition. Applying the concept of Bragg scattering to a randomly rough surface that has been analyzed into Fourier components requires that each component scatter independently and that the total energy scattered from the surface be the summation of the energy scattered by the individual components.

Rice [1951] precisely defined such a surface as 'slightly rough.' It is characterized by height variations that are small compared to the incident wavelength and by slopes that are small compared to unity. By using this formulation, he determined the energy scattered by a slightly rough surface and found it proportional to the two-dimensional energy density spectrum of the surface height variations. Therefore, when viewing a slightly rough surface, a radar may be considered a spatial filter, in that the energy received is primarily proportional to the intensity (square amplitude per unit wave number in the one-dimensional case) of the roughness component whose wave number satisfies the Bragg scattering condition, or, because a number of components may be involved, a Bragg resonance condition. That these considerations apply to waves on the air/water interface has been experimentally verified, first by Crombie [1955] who observed Bragg resonance in wind wave systems and by Wright [1966] who conclusively demonstrated that the radar scattering from mechanically generated water waves in a tank was Bragg scattering. Consequently, the division of the continuous ocean wave spectrum to form a composite is consistent with scattering theory and with measurement because the smaller wave structure

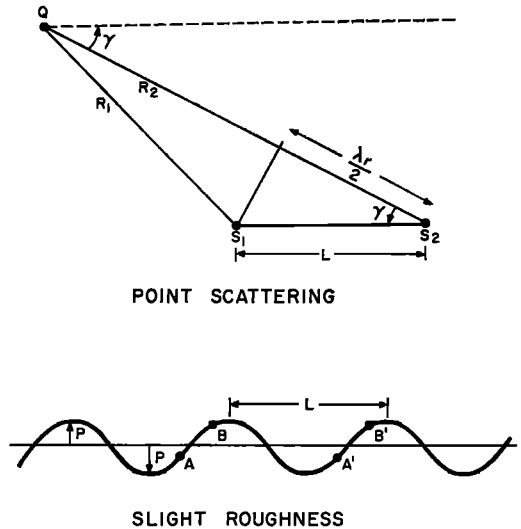


Fig. 2. Bragg scattering geometry.

is chosen to include the portion of the spectrum that may be resonant for a given radar wavelength, whereas the longer waves are chosen to provide a uniform rotation of the scattering surface.

In the analysis of the radar return from area extensive targets, such as the sea, the most useful description is in terms of the NRCS, σ_0 . This parameter is defined as

$$\sigma_0 = \frac{1}{A} \lim_{R \rightarrow \infty} 4\pi R^2 (P_s/P) \quad (3)$$

where R is the range to the scattering surface, P , and P_s are the scattered and incident powers, and A is the area illuminated by the radar. Conventionally, the area has been determined by the intersection of the one-way radar beam pattern with the scattering surface. However, Wright and Keller [1970] and Valenzuela et al. [1970], have recently shown that the two-way beam pattern more accurately measures the illuminated area. For Gaussian-shaped beams, the two-way pattern reduces the area by a factor of 2 (3 db). For beams more steeply sloped than Gaussian the correction introduced by the two-way pattern significantly decreases. To be consistent with previously published data we will adhere to the more conventional definition.

Because the scattering process is normally linear and dependent on the polarization of the incident field, the NRCS can be expressed in

terms of the scattering matrix, an operator that transforms the incident field into the scattered field. Consequently,

$$\sum_0 = \begin{bmatrix} \sigma_{HH} & \sigma_{HV} \\ \sigma_{VH} & \sigma_{VV} \end{bmatrix} \quad (4)$$

where the matrix elements are the NRCS relating a given incident polarization, horizontal or vertical (first subscript) to the scattered polarization (second subscript). Although the matrix elements are in general complex, in calculations of the scattered power only the magnitudes are of interest. To determine the NRCS of the composite surface, *Wright* [1968] temporarily neglected the larger waves and calculated the cross section of the smaller structure, assumed to be a slightly rough surface, by perturbation techniques. He found the NRCS for the directly polarized cases to be of the form

$$\begin{aligned} \sigma_{HH} &= 4\pi\beta^4 \sin^4 \gamma \alpha_{HH} W(K_x, K_y) \\ \sigma_{VV} &= 4\pi\beta^4 \sin^4 \gamma \alpha_{VV} W(K_x, K_y) \end{aligned} \quad (5)$$

$$0 \leq \gamma < \pi/2$$

where K_x and K_y are the wave numbers in the x and y directions on the scattering plane, and W is the two-dimensional energy density spectrum of the surface height variations. The α terms are given by

$$\alpha_{HH} = \left| \frac{(\epsilon - 1)}{[\sin \gamma + (\epsilon - \cos^2 \gamma)^{1/2}]^2} \right|^2 \quad (6)$$

$$\alpha_{VV} = \left| \frac{(\epsilon - 1)[\epsilon(\cos^2 \gamma + 1) - \cos^2 \gamma]}{[\epsilon \sin \gamma + (\epsilon - \cos^2 \gamma)^{1/2}]^2} \right|^2$$

where ϵ is the complex dielectric constant of the surface. Several authors [*Peake*, 1959; *Valenzuela*, 1967; *Bass et al.*, 1968] have achieved a similar result. *Valenzuela* [1967] also determined the value of the cross-polarized elements for the slightly rough surface. Utilizing the Bragg condition and assuming wave propagation in the x, z plane, only components for which

$$K_x = 2\beta \cos \gamma \quad (7)$$

$$K_y = 0$$

are effective in the scattering process.

The rotation of the scattering surface by the larger waves is reintroduced by considering the

effective depression angle of the incident energy to be modified by a rotation in the plane of incidence φ and a rotation in the plane normal to the plane of incident ρ , where the probability distribution of φ and ρ is given by

$$\begin{aligned} P(\varphi, \rho) &= (2\pi S^2)^{-1} \exp \left[-\frac{\tan^2 \varphi + \tan^2 \rho}{2S^2} \right] \end{aligned} \quad (8)$$

where S^2 is the average of the upwind, downwind, and crosswind mean-squared slopes. The value of the average mean-square slope can be determined from the surface wind [*Wright*, 1968] or from the slope spectrum [*Valenzuela et al.*, 1970]. By averaging the values of the NRCS given by (5) as weighted by (8) over the allowable range of rotation angles, the NRCS of the composite surface can be obtained.

A further simplification results if an upper bound on the NRCS is desired. *Phillips* [1966] has defined the equilibrium range of the ocean spectrum as that portion of the spectrum in which waves have been developed to a height that is limited by gravitational constraints. If the Phillip's spectrum (there are other options) is used as a specification of surface roughness, the maximum waveheight condition determines an upper limit (saturation value) of the NRCS of the sea for a given set of illumination parameters. From dimensional arguments, *Phillips* defined the form of the equilibrium range spectrum as

$$W(K) = BK^{-4} \quad (9)$$

where $K = (K_x^2 + K_y^2)^{1/2}$ and $B = 6 \times 10^{-4}$ for short gravity waves. By combining (5), (7), and (9), the saturation values of the NRCS is found to be

$$\begin{aligned} \sigma_{VV} &= 1.5\pi \times 10^{-3} \alpha_{VV} \tan^4 \gamma \\ \sigma_{HH} &= 1.5\pi \times 10^{-3} \alpha_{HH} \tan^4 \gamma \end{aligned} \quad (10)$$

$$0 \leq \gamma < \pi/2$$

Guinard and Daley [1970] found good agreement between the measured values of the direct polarized vertical NRCS and those predicted by (10) over the range of grazing angles from 5°, the lowest angle measured, to 60° from UHF to X band for wind speeds over 5 m/sec. A similarly close fit of theory to experiment for the horizontally polarized values of the NRCS

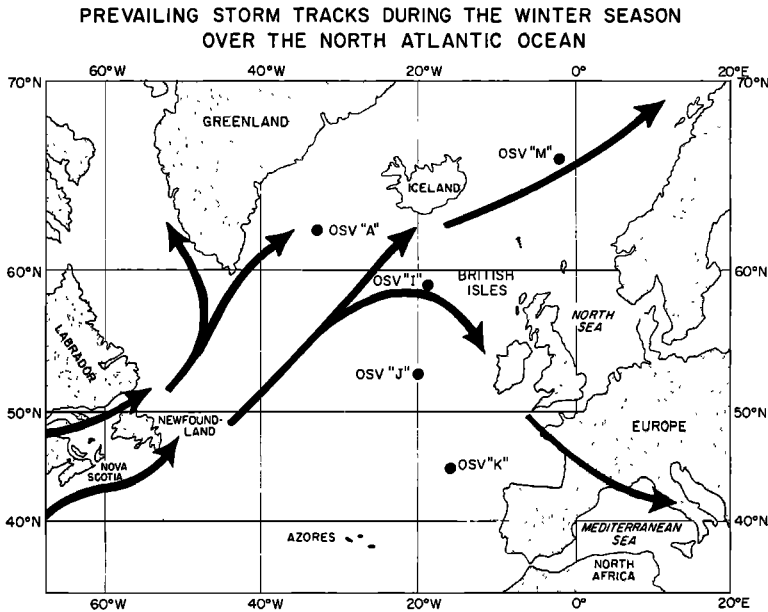


Fig. 3. Prevailing storm tracks during the winter season over the North Atlantic Ocean.

could be obtained at shallow grazing angles only by the introduction, in an ad hoc manner, of the larger waves to 'tilt' the scattering surface. The close approach of the measured values of the NRCS to the saturation value for wind speeds over 5 m/sec strongly showed that the development of the Bragg resonant waves was nearing the maximum condition assumed to exist in the equilibrium range of the ocean spectrum.

HIGH SEA-STATE MEASUREMENT PROGRAM

The close approach to the saturation condition in moderate sea states when considered with the linear assumptions of the slightly rough scattering theory cast considerable doubt on the validity of the model in the higher sea states in which mechanisms involving nonlinear wave interactions, spray, and shadowing would be expected to produce different values of the cross section than predicted. Consequently, we planned to measure the behavior of the sea return in high sea states under conditions in which sufficient surface truth was available to specify growth characteristics of the NRCS with wind and wave height and to provide the sea-state conditions under which saturation of the cross section would occur if it existed. To achieve these objectives, a measurement site was re-

quired at which the probability of observing rough seas was high and, simultaneously, where a source of surface truth could be obtained. We found such a site in the North Atlantic Ocean where in the winter months a storm flow (Figure 3) proceeds south of Labrador, Greenland, and Iceland, across the ocean and along the European coast. As a result, during January and February there is a 30% frequency of wave heights over 4 meters and a 10% frequency of wave heights over 7 meters. Ocean stations India (59°N , 19°W) and Juliet (52.5°N , 20°W) are in the path of these storms on which ocean station vessels, staffed and maintained by the British, Dutch, and French weather services, are located on a rotating schedule. The vessels provide oceanographic and meteorological observations to the international weather services and are equipped with radio beacons to serve as check points for transoceanic flights and, consequently, are almost ideal terminal points for the measurements.

In February 1969, the 4FR System installed in an EC-121 aircraft was deployed to Shannon, Ireland, and during the first 3 weeks of the month, nine missions were flown to ocean stations India and Juliet. The site choice was made dependent on the sea state reported by

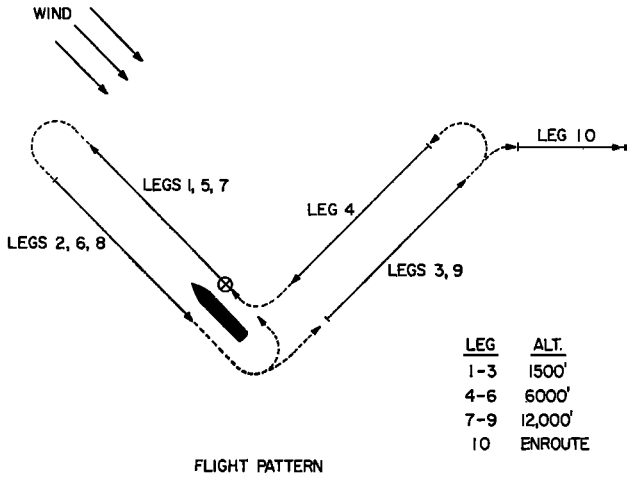


Fig. 4. Flight pattern.

each station and on the meteorological forecast. At the station, the OSV was used as a reference point, and the flight plan shown in Figure 4 was initiated. The plan consists of three legs flown with respect to the wind, up, down, and cross at each of three altitudes and a tenth leg flown on the return. The use of three altitudes is required because of the difficulty of encompassing the entire range of sea return in the radar receiver because gain settings must remain constant to maintain calibration. The altitudes shown in the figure are nominal; the lower altitude was primarily set by visibility of the ocean surface required by the aerial cameras and laser altimetry. On the low altitude legs, data were taken upwind at the shallow grazing angles, 5° through 30° , by fixing the antenna depression angle (the azimuth angle was along the flight path) and recording the return over approximately a 40-sec period, resetting at the next depression angle in the sequence and repeating the procedure until the angular range was covered. The antenna was then rotated 180° in azimuth, the same range of depression angles set, and the return measured. This enabled upwind, downwind data, and data in both directions across the wind to be acquired on each leg. After the upwind leg, a downwind leg and crosswind leg were flown and the measurements were repeated. At the middle altitude, data were collected in a similar manner, from 20° to 60° of grazing angle, where the overlap provided a measure of the constancy of the median cross

section with altitude and time. The angles were similarly overlapped at the higher altitudes. The entire pattern required approximately 2 to 3 hours to finish depending on wind speed, and generally the measurement program began at 1300 UT. The tenth leg shown on the figure was flown on the return flight at constant altitude to evaluate the variation of the cross section in a varying sea condition. Table 1 lists hourly the wind and wave conditions that were reported at the ocean stations for each mission. On seven of the nine missions, data were acquired in sea states in which the wind exceeded 7.5 m/sec, the largest wind condition observed in the Puerto Rico experiment. The maximum sea-state condition was observed on February 11 when an 8.5-meter significant wave height was combined with a 23-24-m/sec wind.

One of the major problems in the measurement of cross section from an airborne platform is the calibration of the radar system. In general, two calibrations are required to eliminate system constants: an internal calibration accomplished by measuring the receiver transfer function from the antenna output terminals to the recording medium by means of standard signal generators and an external calibration to determine the constants related to the antenna gain, radome losses, and radiated power. In the external calibration, 0.2-meter aluminum spheres are used as reference targets of known cross section. These are dropped from the aircraft and tracked manually. Figure 5 is an example of a sphere return.

TABLE 1. Gross Surface Conditions, North Atlantic Ocean, February 1969

	1200 UT		1300 UT		1400 UT		1500 UT		1600 UT	
	Waves	Wind	Waves	Wind	Waves	Wind	Waves	Wind	Waves	Wind
Feb. 6 'T' Sea swell			5m9s 7.7m13s 330°	340/20						
Feb. 8 'J' Sea swell	0.7m3s 4m9s 330°	168/4.5	0.7m3s 4m9s 330°	080/3.5	0.7m3s 4m9s 330°	Calm			0.7m3s 5m9s 330°	110/03
Feb. 10 'T' Sea swell			4m7s 6m10s 260°	240/15.5	4.3m8s 6m10s 240°	240/16.5	4.3m8s 6m10s 240°	240/15	4.3m8s 6m10s 240°	240/17.5
Feb. 11 'T' Sea swell	7m10s 8.7m12s 280°	290/23	7m10s 8.7m12s 280°	290/23	7m10s 8.7m12s 280°	290/24	7m10s 8.7m12s 280°	290/24	7m10s 10m12s 280°	290/26
Feb. 13 'J' Sea swell	7.6m12s	360/19.5	7.6m12s	360/17.5	7.6m12s	360/18	7.6m12s	350/19.5	7.6m12s	360/18.5
Feb. 14 'J' Sea swell	7.6m12s	010/19	8.7m10s	010/20	8.7m10s	010/20	7.6m12s	360/18.5		
Feb. 17 'T' Sea swell	1m3s 3.3m7s 240°	290/08	1m3s 4m7s 240°	240/2.5	1m1s 4m7s 240°	260/2.5	1m1s 4m7s 240°	250/2.5	0 3.3m6s 240°	Calm
Feb. 18 'J' Sea swell	3.3m10s	110/11	3.3m10s	110/11	4m10s	100/11	4m10s	120/13	4m8s	110/11
Feb. 20 'J' Sea swell			5.5m10s	060/14.5	5.5m10s	060/14.5	5.5m10s	050/14		

RADAR ON SEA SURFACE

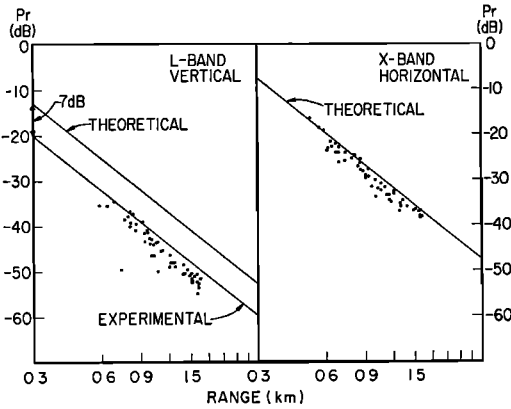


Fig. 5. Typical sphere calibration, North Atlantic, 1969.

The ordinate in this figure is relative amplitude of the return in decibels and the abscissa is the logarithm of the range. The figure is a compilation of several consecutive sphere tracks made before measuring the sea return in the North Atlantic. Each point represents the upper decile value of a 32 pulse sample of the return. The upper decile is used because all errors in sphere tracking tend to lower the observed values of the cross section. The theoretical value of the return shown is computed from the radar equation by using measured transmitter power, the value of the cross section, antenna gain appropriate for the frequency transmitted, and an estimate of the line and radome losses. As the X-band horizontal summary shows, the theoretical value provides an excellent measure of the calibration value for the return. On the other hand, the L-band vertical summary shows a 7-db loss between the theoretical value and the sphere return indicating the need for a 7-db correction to the observed values of cross section. To use this calibration procedure effectively, all cross-sectional values are referenced to the calibration sphere cross section in the following manner. The RCS of the sphere is given by

$$\sigma_s = \frac{(4\pi)^3}{G^2 \lambda^2} \left(\frac{P_{RS}}{P_{TS}} \right) R_s^4 \quad (11)$$

where P_{RS} and P_{TS} are the received and transmitted powers, λ is the radar wavelength, G is the maximum antenna gain, and R_s is the range to the sphere. Applying the same definition to the surface cross section and taking the ratio of σ_T to σ_s gives

$$\sigma_T = \frac{P_{RT}}{P_{RS}} \left(\frac{R_T}{R_S} \right)^4 \sigma_s = A \sigma_s \quad (12)$$

where σ_T is the surface cross section, and P_{RT} is the corresponding radar return. In addition to these calibrations, in view of the many switching operations in the 4FR system, a constant fraction of the transmitted power, termed the reentrant signal, is inserted into each of the microwave input lines and observed at the operator's console to monitor the system performance. The reentrant is periodically recorded with the data to assess system stability. As a result of these calibration procedures, an average accuracy of ± 2 db of cross section is achieved. This value is obtained by monitoring receiver drift and noting the scatter of measurements of the reference sphere when illuminated under optimum conditions.

RADAR RETURN IN HIGH-SEA STATES

Figures 6 through 13 show the comparison between the theoretical limit curves and the data collected in the high-sea states in the North Atlantic by using the 4FR System. The ordinates in these figures are the median values of the statistical distribution of the NRCS observed at fixed depression angle. The sampling rate is the radar pulse repetition frequency, 603 pps, and the range resolution is approximately 80 meters which corresponds to a transmitted pulsewidth of $0.5 \mu\text{sec}$. The values apply to each of the frequency/polarization transmissions. The sample length is approximately 120 sec. The measured values of the NRCS are coded according to windspeed and are the values measured in the upwind direction. The numerals in the parentheses in the legend refer to the February date of the measurement. An over-all view of these data indicates great similarity between the high-sea state returns and those previously reported for the Puerto Rico mission. In particular, a similar good agreement is shown for the vertically polarized cross section in Figures 6 to 8 with both the magnitude and shape of the theoretical limit curve, as was noted previously. On the other hand, the P-band/UHF cross sections in Figure 9, although having a similar trend, have a wider discrepancy in absolute magnitude. This may be the result of the choice of the Phillip's spectrum ($W \sim K^{-4}$) rather than the Kinsman spectrum ($W \sim K^{-3.75}$),

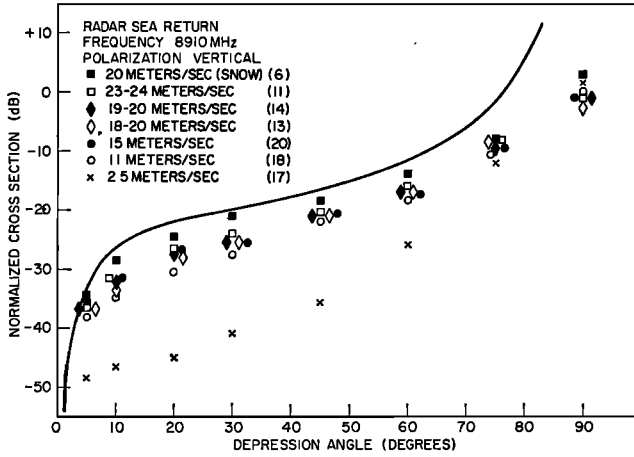


Fig. 6. Radar cross section $\sigma_0(X_{VV})$ for various wind speeds, North Atlantic Ocean, February 1969.

a point discussed in *Guinard and Daley* [1970]. Figures 10 through 13 are the collations using the horizontally polarized cross sections for the various frequency transmissions. These exhibit to a high degree the influence of the large wave structure in tilting the scattering surface and are in general agreement with the theoretical predictions with this proviso.

One of the more fortunate occurrences in this experiment was the low-sea state condition encountered on February 17 that provides a common wind condition with the NRCS data acquired in Puerto Rico and thus allows certain conclusions to be drawn on the variation of

cross section with wind. Neglecting February 6 on which anomalous results were obtained and which will be discussed later, wind variation is radically different in the lower frequency NRCS than in the higher frequency at the shallower grazing angles. Referring to the *L*-band and *P*-band/UHF returns in Figures 8, 9, 12, and 13, there is an increase of approximately 5 or 10 db, depending on the choice of frequency and angle, in the observed cross section for an increase in wind speed from 2.5 to 24 m/sec. This is to be contrasted with the increase in cross section with wind in the *X*- and *C*-band data shown in Figures 6, 7, 10, and 11, in which nearly 20 db

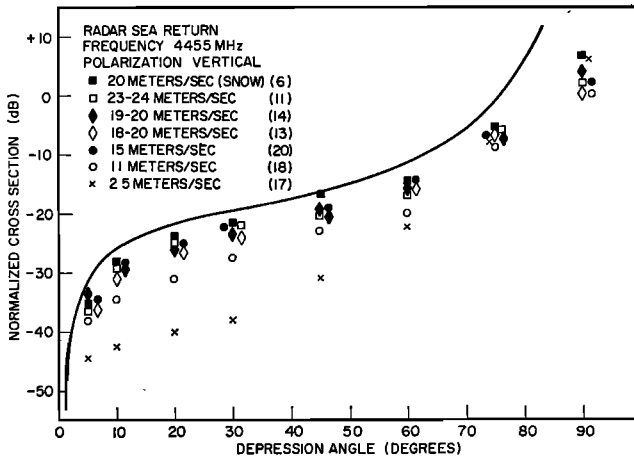


Fig. 7. Radar cross section $\sigma_0(C_{VV})$ for various wind speeds, North Atlantic Ocean, February 1969.

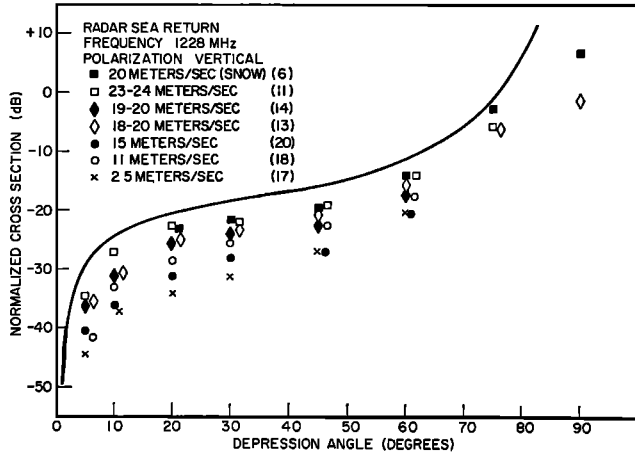


Fig. 8. Radar cross section $\sigma_0(L_{VV})$ for various wind speeds, North Atlantic Ocean, February 1969.

is shown. Such behavior is consistent with the mechanisms implied by the composite surface theory. For X- and C-band transmissions over the grazing angle range from 5° to 60°, the scattering wavelengths lie in the unstable region in the vicinity of the null in the wave velocity dispersion relationship, and thus their height is strongly influenced by the presence of wind. The resonant scatterers for the L-band and P-band/UHF radiation, however, lie well in the small gravity wave spectrum and are far less sensitive to local wind.

The mission of February 6 was unique in the North Atlantic series because there were inter-

mittent snow falls, gusting winds, and a positive sea/air temperature difference over the measurement area. The values of the NRCS obtained were the highest, or among the highest, acquired. In view of the variation of NRCS with wind-speed observed in the other missions, it is hard to assign the high values to wind phenomena. Another possible mechanism is surface roughening by the snow; however, the intermittence of the snow falls and the absence of a strong frequency dependence in the NRCS make this explanation unlikely. The sea/air temperature difference does offer a plausible explanation for the observed phenomena. The effect of insta-

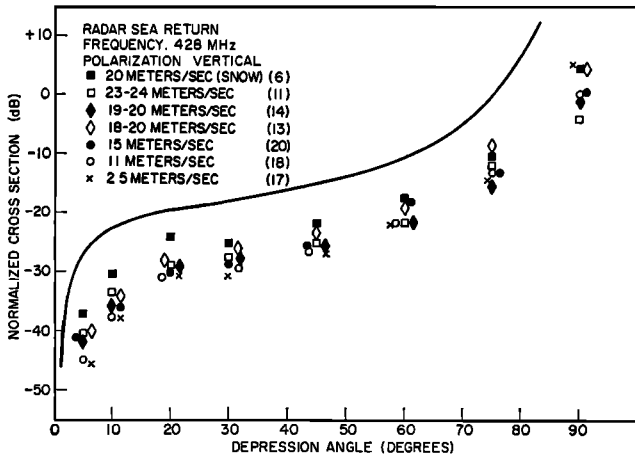


Fig. 9. Radar cross section $\sigma_0(P_{VV})$ for various wind speeds, North Atlantic Ocean, February 1969.

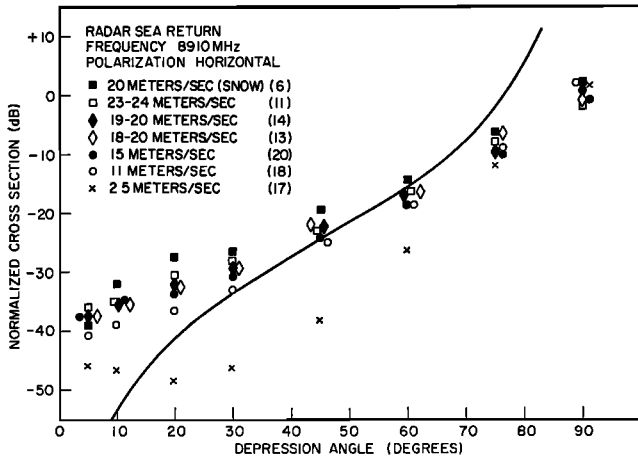


Fig. 10. Radar cross section $\sigma_0(X_{HH})$ for various wind speeds, North Atlantic Ocean, February 1969.

bility at the sea/air interface on wave height has been observed by *Brown* [1953]. His measurements indicate that, for a given wind speed, the mean wave height increases particularly with positive sea/air temperature difference at the higher wind speeds (data to Beaufort Force 6). The wind at the site recorded by the OSV was Beaufort Force 8; consequently the anomalous data acquired on February 6 can be attributable to this effect. If this mechanism can be firmly established, it will have great bearing on the remote sensing of wind fields by radar because the effect on the cross section of the

temperature difference is equivalent to a change in wind speed from 5 to 20 m/sec.

It is interesting to attempt to determine the growth of NRCS with wind in a more precise manner to determine at which point the saturation value is closely approached and to explore the possibility of using NRCS as a measure of local wind fields. Figures 14 and 15 show the growth of the NRCS with wind for X-band returns at 30° depression angle for both polarizations of the return. These were compiled by using data from the Puerto Rico and North Atlantic missions. The angle and frequency

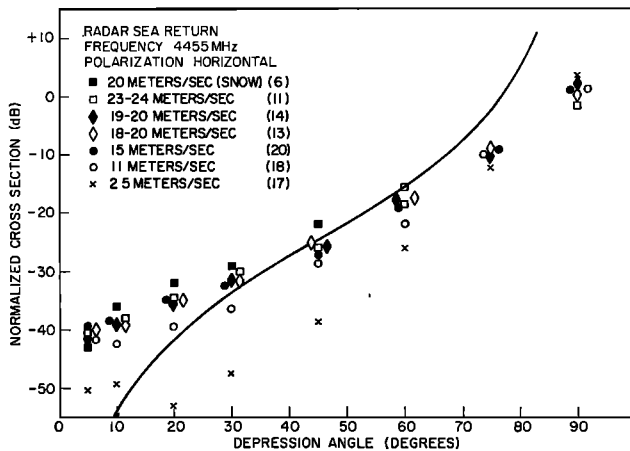


Fig. 11. Radar cross section $\sigma_0(C_{HH})$ for various wind speeds, North Atlantic Ocean, February 1969.

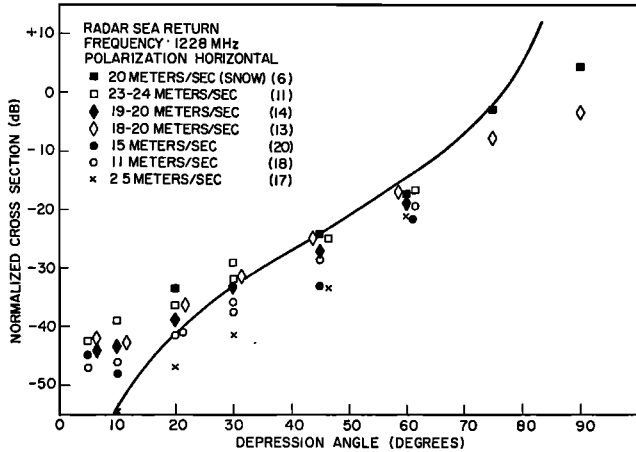


Fig. 12. Radar cross section $\sigma_0(L_{HH})$ for various wind speeds, North Atlantic Ocean, February 1969.

chosen offer the widest variation of NRCS with wind and thus provide a conservative estimate of the location of the saturation region and, simultaneously, optimum conditions for wind speed sensing. To describe the variation two power laws that effectively separate the function into two domains have been fitted to the data. For low wind speeds, a cube law [Long, 1965] provides a good fit to the data, whereas for the higher wind range a square-root law seems to offer a better fit. Similar fitting occurs for each polarization because each depends on the wave spectrum in the same way. In the first domain, 0 to 5 m/sec, the growth of wave height with wind is rapid, whereas in the second, 5 to

24 m/sec, the wave height grows more slowly, asymptotically, to the equilibrium range value, while the NRCS approaches its saturation value. Further measurements are planned to further explore the variation of the NRCS with wind in the critical region between 2.5 and 10 m/sec.

CONCLUSIONS

A study has been undertaken at the Naval Research Laboratory to validate the composite surface model for the NRCS of the sea that had been developed by scientists in both the United States and the Soviet Union in parallel efforts. This was done by collating the values predicted by the model with data collected in a variety of

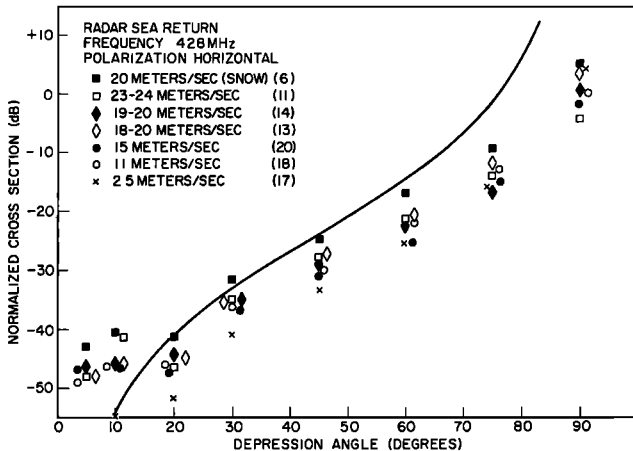


Fig. 13. Radar cross section $\sigma_0(P_{HH})$ for various wind speeds, North Atlantic Ocean, February 1969.

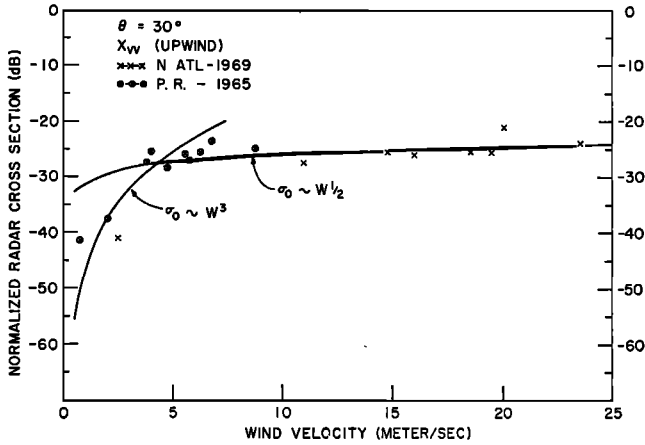


Fig. 14. Variation of radar cross section $\sigma_0(X_{VV})$ with wind speed.

sea conditions by the 4FR System, which is a multiple frequency dual polarized airborne radar. The comparison has shown that the theory closely predicts the variation of the NRCS with frequency and grazing angle for the vertically polarized returns. However, the horizontally polarized returns are fitted in the region of low grazing angles only by the introduction of the sea swell in an ad hoc manner as a 'tilting' of the scattering surface. To validate the theory under conditions in which mechanisms involving spray and nonlinear wave interaction and shadowing which were neglected in the calculation would be expected to be dominant and to determine a worst-case condition for the radar sea return, an experiment was con-

ducted in February 1969 in the North Atlantic Ocean in high-sea states. As a result of this measurement, data are now available for the variation of sea cross section with grazing angle over the range from 5° to 90° for frequencies from UHF to X band with both linear polarizations in sea states ranging from 0 to 7. A maximum condition of a 24 m/sec wind with 8.5 meter significant wave height was observed.

These data have been also collated with the composite surface theory and validate the predictions of the theory and give further indication of the 'tilting' of the scattering surface by long waves. Lastly, the data collected with the X-band system at 30° grazing angle have been used to determine an optimistic estimate of the

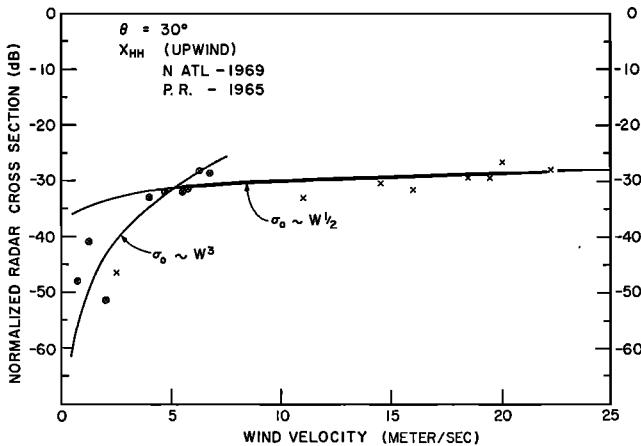


Fig. 15. Variation of radar cross section $\sigma_0(X_{HH})$ with wind speed.

variation of the NRCS with wind and a conservative estimate of the wind speed at which saturation is approached.

Acknowledgments. We wish to acknowledge the assistance and advice of Dr. G. Valenzuela and Dr. J. Wright in the treatment of the composite surface model, to Mr. Lionel Moskowitz for his assistance in planning the experiment and providing surface truth, and to the 4FR team without whom there would be no data to report.

REFERENCES

- Barrick, D. E., and W. H. Peake, A review of scattering from surfaces with different roughness scales, *Radio Sci.*, **3**(8), 865, 1968.
- Bass, F. G., I. M. Fuks, A. I. Kalmykov, I. E. Ostrovsky, and A. D. Rosenberg, Very high frequency radiowave scattering by a disturbed sea surface, *IEEE Trans. Antennas Propagat.*, **16**(5), 554, 1968.
- Brown, P. R., Wave data for the eastern North Atlantic, *Mar. Obs.*, **23**(160), 94, 1953.
- Crombie, D. D., Doppler spectrum of sea-echo at 13.56 mc/s, *Nature*, **175**, 681, 1955.
- Guinard, N. W., The NRL four-frequency radar system, Report of NRL Progress, May 1969.
- Guinard, N. W., and J. C. Daley, An experimental study of a sea clutter model, *IEEE Proc.*, **58**(4), 543, 1970.
- Long, M. W., R. D. Wetherington, J. L. Edwards, and A. B. Abeling, Wavelength dependence of sea echo, *Georgia Inst. Tech. Final Rep. Proj. A-840*, p. 31, 1965.
- Peake, W. H., Theory of radar return from terrain, *IRE Nat. Conv. Rec.*, **7**, pt. 1, 27, 1959.
- Phillips, O. M., *The Dynamics of the Upper Ocean*, 109-113 Cambridge University Press, London, 1966.
- Rice, S. O., Reflection of electromagnetic waves from slightly rough surfaces, *Comm. Pure Appl. Math.*, **4**(2/3), 351, 1951.
- Semyonov, B. J., An approximate calculation of scattering from the perturbed sea surface, *IVUZ Radiofiz. (USSR)*, **9**, 876, 1966.
- Valenzuela, G. R., Depolarization of em waves by slightly rough surfaces, *IEEE Trans. Antennas Propagat.*, **15**(4), 552, 1967.
- Valenzuela, G. R., M. B. Laing, and J. C. Daley, Ocean spectra for the high frequency waves from airborne radar measurements, *J. Mar. Res.*, **29**, in press, 1971.
- Wright, J. W., Backscattering from capillary waves with application to sea clutter, *IEEE Trans. Antennas Propagat.*, **14**(6), 749, 1966.
- Wright, J. W., A new model for sea clutter, *IEEE Trans. Antennas Propagat.*, **16**(2), 217, 1968.
- Wright, J. W., and W. C. Keller, Doppler spectra in microwave scattering from wind waves, *Phys. Fluids*, **14**(2), 1971.

(Received April 23, 1970;
revised November 23, 1970.)